Velocity estimation on an active suspension for a translational electrodynamic maglev system

Velocity Estimation on an Active Suspension for a Translational Electrodynamic Maglev System

Eugenio TRAMACERE[a], Marius PAKŠTYS[a], Luis Miguel CASTELLANOS[a], Renato GALLUZZI[b], Lorenzo BOSICA[a], Nicola AMATI[a], Andrea TONOLI[a],

a Department of Mechanical and Aerospace Engineering, Politecnico di Torino, 10129 Torino, Italy eugenio.tramacere@polito.it
b School of Engineering and Sciences, Tecnologico de Monterrey, Calle del Puente 222, Mexico City, 14380, Mexico

Abstract

The concept of Hyperloop was proposed over a decade ago. Since then, numerous efforts have focused on improving this technology towards commercial applications. Although promising, the electrodynamic levitation system is inherently unstable. However, instability can be mitigated by the introduction of a secondary suspension between the capsule and the bogie. To evaluate stabilization strategies, a dedicated test bench has been constructed. Nevertheless, these methods require a reliable estimation of the relative velocity between the capsule and the bogie for their successful practical implementation. This work focuses on the estimation of this velocity using a Kalman filter approach based on an augmented model of the electrical circuit of a voice coil actuator, which constitutes the secondary suspension of the presented electrodynamic levitation system. The proposed approach has been implemented and tested on a real-time ECU, demonstrating the capability of the method for applications involving active damping control.

Keywords: Hyperloop, electrodynamics, levitation, Kalman filter, velocity estimation

1. Introduction

The Hyperloop concept has emerged in the last decade as an ultra-high speed transportation system, with potentially low emissions. Urban connectivity as well as freight transportation may see overall improvements in terms of travel and lead time, motivating a research interest in this technology. The core operating principle exploited is passive electrodynamic levitation, where an array of permanent magnets interacts with the non-ferrous conductive track due to their relative translational velocity. Eddy currents generated in the track result in lift and drag forces experienced by the levitating pad. However, this levitation phenomenon is inherently unstable, and stability has been numerically achieved by introducing a secondary suspension that ensures a two degree of freedom (DOF) configuration (Galluzzi et al. (2020)).

A test bench has been constructed to study this electrodynamic levitation system, allowing for the validation of proposed control strategies. It is characterized by a copper ring mounted on an aluminium disk coupled to a brushless servomotor by means of a mechanical joint. The disk is oriented with its spinning axis vertical, so as to ensure a small footprint. The test bench structure is composed of transparent panels, and a cavity permitting equipment installation. Such equipment is constituted by two masses installed onto a micro-metric stage as shown in Figure 1a. The masses can be identified as per the equivalent quarter car model in Figure 1b: the sprung mass m_s associated with the capsule of a maglev train and the unsprung mass m_{us} associated with the bogie. Horizontal or lateral movement is prevented by flex hinges, which only permit vertical displacement. A first set of flex hinges connects the unsprung mass to the frame of the test bench (equivalent stiffness k_u). A second set of flex hinges is installed between the sprung and the unsprung masses (equivalent stiffness k_s). The combination of these flex hinges and a voice coil actuator (VCA) with an equivalent damping c_s constitutes the secondary suspension.

For a commercial application of this technology, passenger comfort must be guaranteed. The VCA provides

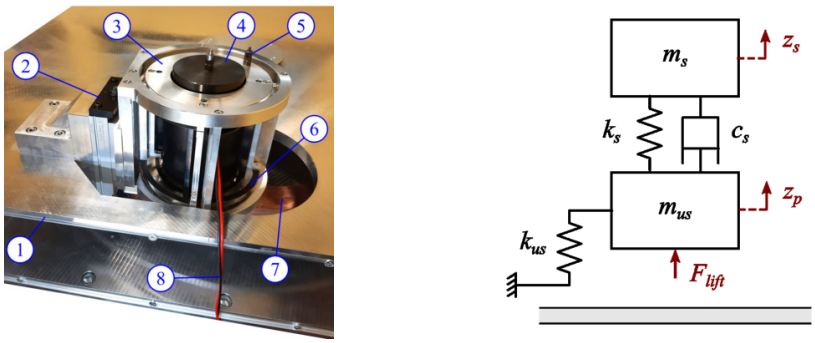

(a) *(b)*

Figure 1: Experimental test bench. (a) Rig setup constituted by (1) support structure; (2) micrometric stage; (3) unsprung mass; (4) sprung mass; (5) accelerometer [x2]; (6) flex hinges; (7) copper track; (8) voice coil winding terminals. (b) Equivalent quarter car model.

the possibility of implementing passive or active control, such that the oscillations of the sprung mass are attenuated. Passive control involves supplying a load-relieving voltage to the VCA, and exploiting the intrinsic damping due to eddy current generation in the structure of the actuator. In the studied application, the VCA functions as a passive damper. Active and semi-active control is of greater interest as several control strategies can be introduced to significantly improve comfort (Zhang (2019)). The Linear Quadratic Regulator (LQR) falls under an active control scheme, while the skyhook controller is a potential semi-active control strategy (Negash et al. (2021)). For their practical implementation in the context of the VCA, a reliable estimation of relative velocity between the sprung and the unsprung masses is required.

This work focuses on the estimation of the relative velocity using a Kalman filter approach, incorporating an augmented numerical model of the VCA. The use of a Kalman filter with a LQR control strategy is explored for active magnetic bearings by Schuhmann et al. (2006), demonstrating the potential for active control in a system with similar operating principles. A single measured variable is necessary for the Kalman filter to estimate relative velocity. Electrical dynamics of the VCA can be exploited to estimate the relative velocity in a sensorless approach. Noise in the estimation must be considered to verify the viability of the aforementioned approaches in active control strategies.

The remainder of the paper is organized as follows. Section 2 outlines the numerical method used to implement the Kalman filter. Section 3 shows the experimental results for the relative velocity estimation. Finally Section 4 concludes the work.

2. Method

The numerical model adopted to estimate the relative velocity between the two masses is represented by the electrical circuit of the VCA. The electrical domain of a voice coil actuator can be represented by a simple series circuit with impedance terms R_{vc} and L_{vc}, input voltage source V and a back electromotive force (back-EMF) $E_{vc} = K_v(\dot{z}_s - \dot{z}_p)$, where $\dot{z}_s$ represents the velocity of the sprung mass and $\dot{z}_p$ represents the velocity of the unsprung mass. Kirchhoff's voltage law is applied to the electric circuit of the VCA:

$$V = L_{vc}\frac{\mathrm{d}i_{vc}}{\mathrm{d}t} + R_{vc}i_{vc} + E_{vc} \tag{1}$$

During testing, the VCA is controlled with a voltage input applied by a TI™ F28379D LaunchPad™ card and a TI™ BOOSTXL DRV8323RS power stage. The current across the VCA is measured by a current sensor, as shown in Fig. 2. Subsequently, the measured current is processed in real-time by the dSPACE™ MicrolabBox that calculates the back-EMF value through Eq. 1. The disadvantage of this method is the use of the derivative of

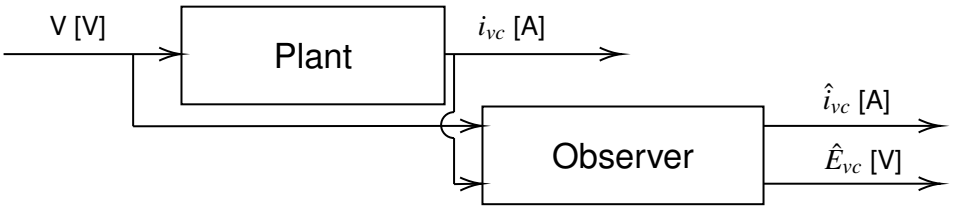

Figure 2: Scheme of the proposed observer.

the measured current which introduces noise in the calculated back-EMF signal. Using this signal as a feedback variable for active damping control may result in sub-optimal vibration attenuation.

Therefore, a disturbance observer based on Kalman filter is designed to suppress model parameter uncertainty and an external disturbance signal, as Figure 2 shows. Assuming the induced voltage E_{vc} as a disturbance with zero derivative (Chappuis et al. (2015)), the following expression can be written:

$$\frac{d}{dt}E_{vc} = 0 \tag{2}$$

The derivative of the back-EMF tends to zero because it is assumed that the relative velocity variation due to the mechanical dynamics of the electrodynamic levitation system is slower than the electrical dynamics of the VCA. Thus, the induced voltage, coupled with the relative velocity variable through the VCA velocity constant K_v, has a quasi-static behavior.

A continuous state space representation based on Eqs. 1 and 2 is assembled. The state vector ξ in Eq. 3 contains the voice coil current i_{vc} and the induced voltage E_{vc}. The input vector u in Eq. 4 contains voltage across the VCA terminals V. The output vector y in Eq. 5 contains VCA current. The dynamic matrix A_c, input gain matrix B_c, output gain matrix C, and direct link matrix D in Eqs. 6, 7, 8, and 9 describe the augmented system.

$$\xi = \{i_{vc} \;\; E_{vc}\}^{\mathsf{T}} \tag{3}$$

$$u = \{V\} \tag{4}$$

$$y = \{i_{vc}\} \tag{5}$$

$$A_c = \begin{bmatrix} -\frac{R_{vc}}{L_{vc}} & -\frac{1}{L_{vc}} \\ 0 & 0 \end{bmatrix} \tag{6}$$

$$B_c = \begin{bmatrix} \frac{1}{L_{vc}} & 0 \end{bmatrix}^{\mathsf{T}} \tag{7}$$

$$C = \begin{bmatrix} 1 & 0 \end{bmatrix} \tag{8}$$

$$D = \begin{bmatrix} 0 \end{bmatrix} \tag{9}$$

The augmented plant model can thus be introduced into the observer model. Equation 10 refers to the observer, from which the filter can be obtained. The dynamic matrix $\bar{A}$, input gain matrix $\bar{B}$, output gain matrix $\bar{C}$, and direct link matrix $\bar{D}$ in Eqs. 14, 15, 16, and 17 represent the state space of the Kalman filter. Note that the Kalman gain K_f is constructed with reference to the plant output. The plant output y identifies the measurement input of VCA current for the Kalman filter. Observer states $\hat{\xi}$ in Eq. 12 are identical to plant states, while the inputs $\bar{u}$ in Eq. 13 consist of the VCA voltage and the measured current $\hat{i}_{vc}$. The outputs y contain the estimated states as it is shown in Eq. 16. Finally, the relative velocity estimation v_{rel} can be obtained due to its dependency

on the VCA velocity constant K_v as Eq. 18.

$$\dot{\hat{\xi}} = A\hat{\xi} + Bu + K_f(y - (C\hat{\xi} + Du)) \tag{10}$$

$$= \bar{A}\hat{\xi} + \bar{B}\bar{u} \tag{11}$$

$$\hat{\xi} = \{\hat{i}_{vc} \ \hat{E}_{vc}\}^{\intercal} \tag{12}$$

$$\bar{u} = \{V \ i_{vc}\}^{\intercal} \tag{13}$$

$$\bar{A} = A - K_f C \tag{14}$$

$$\bar{B} = \begin{bmatrix} B - K_f D & K_f \end{bmatrix} \tag{15}$$

$$\bar{C} = \begin{bmatrix} 1 & 0 \\ 0 & 1 \end{bmatrix} \tag{16}$$

$$\bar{D} = \begin{bmatrix} 0 & 0 \\ 0 & 0 \end{bmatrix} \tag{17}$$

$$v_{rel} = \dot{z}_s - \dot{z}_p = \frac{\hat{E}_{vc}}{K_v} \tag{18}$$

Noises associated to states and to measurements are considered in the covariance matrices Q and R as tuning factors:

$$Q = \begin{bmatrix} w_i^2 & 0 \\ 0 & w_E^2 \end{bmatrix} \tag{19}$$

$$R = v_i^2. \tag{20}$$

The weighting parameter w_i refers to noise on the estimated current. Noise on the measured current is considered by the weighting parameter v_i. The weighting parameter w_E refers to noise on the back-EMF. The Kalman estimator in Eq. 10 computes a state estimate $\hat{\xi}$ that minimizes the steady-state error covariance. The proposed filter has been discretized with a sample time of 2 ms and deployed onto the dSPACE™ MicrolabBox on which the relative speed measurement from the RL circuit and the estimate deriving from the Kalman filter can be compared in real-time. The chosen working frequency of 5 kHz ensures a reliable communication between the LaunchPad™ and the MicrolabBox, without incurring overruns. To reduce measurement noise, the analog current signal from the current sensor is acquired by the MicrolabBox synchronously when the H-bridge leg of the LaunchPad™ power stage is closed. Table 1 summarises all parameters necessary for the practical implementation of the discrete Kalman filter.

Table 1: Kalman filter parameters.

Parameter	**Value**	**Unit**
R_{vc}	1.8	Ω
L_{vc}	0.0152	H
K_v	25	Vs/m
w_i	0.001	A
w_E	0.0075	V
v_i	0.001	A

3. Results

Both methods based on back-EMF calculation and the Kalman filter estimation have been tested. The test is performed at a constant disk speed of 500 rpm. The two-mass system is positioned on the micrometric

stage such that the flex hinges for the sprung and the unsprung masses do not exhibit any pre-deformation. Furthermore, the VCA operates by applying an offset voltage that causes the separation of the two masses. Figure 3 shows the measured current i_{vc} (black solid line) and the estimated current from the Kalman filter $\hat{i}_{vc}$ (red dotted line), highlighting the estimated current is completely based on the measured signal. The oscillation of the current with a period of approximately 8 Hz is caused by the periodicity of the irregularities in the copper track, which induces system oscillations with a frequency proportional to the rotor's speed.

Figure 4 shows a comparison between the relative speed measurement using the VCA electrical equation and the Kalman filter's estimated output. A relative velocity signal obtained from accelerometer sensors is also plotted, confirming the results obtained through both estimation methods. The relative velocity signal estimated by the Kalman filter is smooth and filtered, indicating the suitability of the proposed approach for active control. The weighting parameters w_i, w_E and v_i are treated as adjustable parameters. An increase in the ratio between w_i and w_E makes the filter slower in estimating the disturbance, while an increase in the ratio between v_i and w_E makes the estimator less sensitive to the output noise (Castellanos Molina (2020)). The obtained results show a good trade-off in balancing the three weighting parameters. Indeed, the RMS value of the error between the Kalman filter estimation and the RL estimation is 0.0024 m/s. Moreover, the maximum absolute error between the two estimations is 0.0077 m/s.

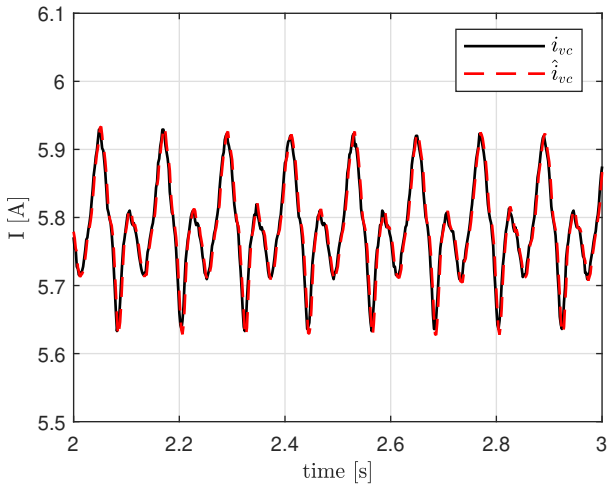

Figure 3: Current measured signal i_{vc} (black solid line) compared with the estimated current state from the Kalman filter $\hat{i}_{vc}$ (red dotted line).

4. Conclusions

The paper proposes a Kalman filter for relative velocity estimation of an electrodynamic levitation system with a VCA working as a secondary suspension system between the capsule and the bogie. The estimator is based on an augmented model of the electrical circuit of the VCA. Due to the augmented state, a relative velocity estimation with less noise compared to the calculation derived from the RL circuit can be achieved. Therefore, the relative speed signal can be fed back to close active damping control loops, i.e. reducing acceleration peaks on the sprung mass for comfort reasons. However, the proposed approach raises critical concerns. The relative speed estimation is accurate provided that the VCA's parameters do not change. Unfortunately, the VCA's resistance tends to increase during operation time. Moreover, the VCA's inductance changes too due to transient operations introduced by the irregularities of the copper track, thus meaning the proposed method does not compensate for plant model mismatches. Future research may employ an Extended Kalman filter strategy or real-time model identification approaches to counterbalance plant uncertainties and disturbances.

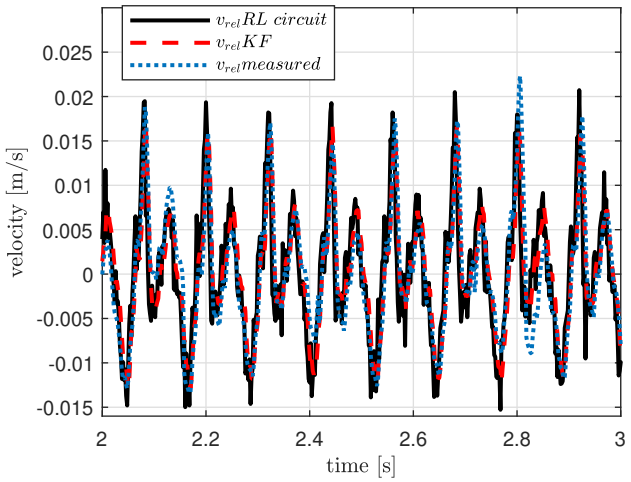

Figure 4: Relative velocity signal comparison between VCA RL circuit method (black solid line) and the Kalman filter approach (red dotted line).

References

Castellanos Molina, L. M. (2020), Offset-Free Model Predictive Control for Active Magnetic Bearings, PhD thesis, Politecnico di Torino.

Chappuis, B., Gavin, S., Rigazzi, L. & Carpita, M. (2015), 'Speed control of a multiphase active way linear motor based on back emf estimation', *IEEE Transactions on Industrial Electronics* **62**(12), 7299–7308.

Galluzzi, R., Circosta, S., Amati, N., Tonoli, A., Bonfitto, A., Lembke, T. A. & Kertész, M. (2020), 'A multi-domain approach to the stabilization of electrodynamic levitation systems', *Journal of Vibration and Acoustics* **142**(6), 061004.

Negash, B. A., You, W., Lee, J., Lee, C. & Lee, K. (2021), 'Semi-active control of a nonlinear quarter-car model of hyperloop capsule vehicle with skyhook and mixed skyhook-acceleration driven damper controller', *Advances in Mechanical Engineering* **13**(2), 1687814021999528.

Schuhmann, T., Hofmann, W. & Werner, R. (2006), 'Adaptive linear and extended kalman filter applied to amb with collocated position measuring'.

Zhang, Z. (2019), 'Applied adaptive controller design for vibration suppression in electromagnetic systems', *The Applied Computational Electromagnetics Society Journal (ACES)* pp. 567–576.